J Therm Anal Calorim (2010) 102:193–201
DOI 10.1007/s10973-009-0382-z

Drug-excipient compatibility studies in binary and ternary mixtures by physico-chemical techniques

Giovanna Bruni · Vittorio Berbenni · Chiara Milanese · Alessandro Girella · Amedeo Marini

Received: 30 April 2009 / Accepted: 22 July 2009 / Published online: 28 August 2009

Abstract This work is part of a systematic study undertaken to find and optimize a general method of detecting the drug-excipient interactions, with the aim of predicting rapidly and inexpensively the long term stability of a pharmaceutical product and speed up its marketing. Here, in particular, the compatibility of haloperidol with several excipients (PVP, magnesium stearate and α-lactose) in binary and ternary mixtures, both as prepared and ball-milled, has been assessed by thermal methods, electron microscopy, IR spectroscopy and X-ray diffraction. The differences between the experimental behaviour of the systems and that expected as weighted average of similarly treated pure components are interaction indicators. The DSC has proven to be, among the selected analytical techniques, the most sensitive and specific in assessing the compatibility. A strong interaction has been observed between PVP and haloperidol. It is favoured by the mechanical stress and is more evident in the composition 20:80. On the contrary, α-lactose and magnesium stearate were found to be compatible with the drug.

Keywords Compatibility · DSC · Haloperidol · Interaction · Thermal analysis

Introduction

In the formulation of a new solid drug, the suitable excipients are selected on the basis of the technological properties of the powder, of the required drug delivery kinetics and of their compatibility with the drug. Compatibility studies are, therefore, a key step in accelerating drug development. Subsequent changes in the formulation as a result of unexpected stability problems lead to an increase in the time and in the cost of drug development. The chance of using a fast and reliable method for the prediction of drug-excipient interaction remains an open problem for the pharmaceutical industry [1–7].

In our previous works [8–11], we proposed a method, to investigate drug-excipient interactions, which makes use of several techniques: it has been shown that DSC is the best technique in the search of interaction indicators. Indeed, with a proper selection of experimental conditions DSC is able to reveal the thermal changes which can result from an interaction between the components in solid phase. Thus, it is possible to detect compatibility directly on the mixtures, without the time consuming step of annealing under stress conditions. Furthermore, we [8–11] put into evidence that the water vapour is an important factor which can induce an interaction between the powders.

The present work is aimed to test the predictive ability of the proposed method with a system containing, as a model drug, haloperidol, an antipsychotic agent. Investigations have been extended from binary to ternary mixtures and the effects of mechanical activation on the interaction have been considered.

Experimental

Haloperidol (99% purity) from Sigma-Aldrich has been used. The commercial grade excipients are PVP (average molecular mass 50,000 amu), magnesium stearate and α-lactose monohydrate. All samples and their mixtures

G. Bruni (✉) · V. Berbenni · C. Milanese · A. Girella · A. Marini
C.S.G.I. – Dipartimento di Chimica Fisica "M. Rolla", Università degli Studi di Pavia, Viale Taramelli 16, 27100 Pavia, Italy
e-mail: bruni@matsci.unipv.it

have been stored in closed plastic containers. Physical mixtures have been prepared by mixing the components in a turbula (W. A. Bachofen) at 96 rpm for 20 min. Binary mixtures have two different compositions: drug:excipient 20:80 and 80:20 by mass. The compositions of ternary mixtures (drug:excipient$_1$:excipient$_2$) are 20:40:40 and 80:10:10 by mass. Measurements were performed on samples prepared as described and on samples ball milled (BM samples) in a planetary mill (Pulverisette 7, Fritsh) for 2 h at 500 rpm (no ball milling was performed on samples containing magnesium stearate).

Thermal measurements were performed with a TGA 2950 thermogravimetric analyzer and a DSC 2920 apparatus (TA Instruments, USA) both interfaced with a TA 3100 data station. In DSC, standard open pans of aluminium have been used as sample holder and reference. Samples have been analyzed under a flow (3 L h^{-1}) of dry nitrogen and of nitrogen bubbled through water at room temperature (wet nitrogen) with scanning rates (β) of 2 and 10 K min^{-1}. At least three replicates of each measurement have been performed. SEM micrographs were collected with a Cambridge Stereoscan 200 on gold-sputtered samples. Diffuse reflectance FT-IR spectra have been collected (4,000–400 cm^{-1}) by a FT-IR system (Nicolet) equipped with a diffuse reflectance cell (DRIFT collector, Spectra Tech, UK). Each sample has been dispersed in about 500 mg of anhydrous KBr (97% in mass) and the resulting powder was ground in an agate mortar.

X-ray diffraction (XRD) patterns have been recorded in air at room temperature with a powder X-ray diffractometer Bruker D5005 connected to a goniometer and a graphite bent crystal monochromator (CuK$_\alpha$ radiation). Measurements were performed in the angular range 5 - 35°2ϑ in the step scan mode (step width: 0.02°2ϑ).

Results

Pure components

Haloperidol

Haloperidol is constituted by flattened particles of roughly hexagonal form and with the major dimension in the order of 300 μm (Fig. 1a). The DSC curve (Fig. 2) shows a sharp endothermic peak due to the melting (onset temperature: 152.3 °C; enthalpy change: 148.4 ± 2.5 J g^{-1}). Such a peak is unaffected either from the heating rate and from the relative humidity in the DSC cell. TG measurements show no mass change from room temperature to 180 °C (maximum temperature of the measurements) so demonstrating that haloperidol does not undergo decomposition under the melting.

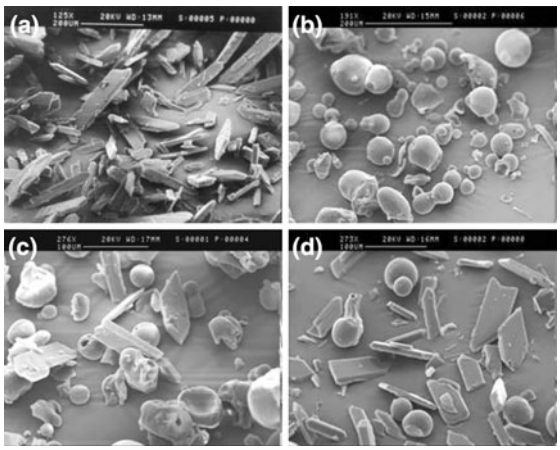

Fig. 1 SEM pictures of haloperidol (**a**), PVP (**b**), haloperidol:PVP = 20:80 (**c**) and haloperidol:PVP = 80:20 (**d**)

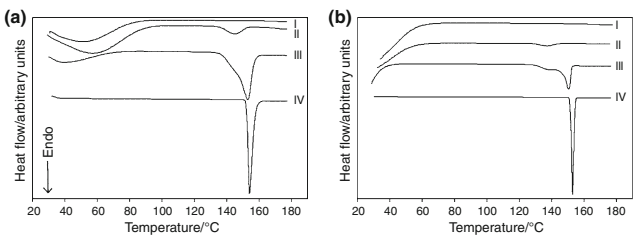

Fig. 2 DSC curves of the system haloperidol:PVP in dry nitrogen at 10 K min^{-1} (**a**) and 2 K min^{-1} (**b**). Curve I: PVP; curve II: mixture haloperidol:PVP = 20:80; curve III: mixture haloperidol:PVP = 80:20; curve IV: haloperidol

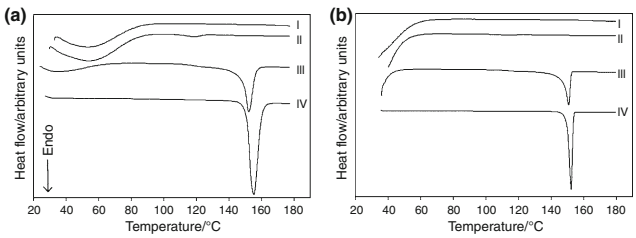

Fig. 3 DSC curves of the high-energy milled system haloperidol:PVP in dry nitrogen at 10 K min^{-1} (**a**) and 2 K min^{-1} (**b**). Curve I: BM PVP; curve II: BM haloperidol:PVP = 20:80; curve III: BM haloperidol:PVP = 80:20; curve IV: BM haloperidol

When subjected to high energy milling, haloperidol shows the break-down of most of its particles so that they loose their hexagonal form. The DSC curve (Fig. 3) shows an endothermic peak again that, however, shifts to at a lower temperature (onset temperature: 150.4 °C) and with a lower associated enthalpy (135.7 ± 4.1 J g^{-1}). The XRD analysis puts into evidence that both the relative intensities and the HWHM of the diffraction peaks change even if the relevant angular position does not appear to be sensibly affected by

milling: this fact allows one to conclude that the differences in the melting peak do not reflect the formation of a new crystalline phase but simply the partial amorphization of the powder.

PVP

PVP powder consists of rounded, smooth particles of diameter up to 100 μm with holes on the surface (Fig. 1b). It has also to be noted that some of PVP particles are broken and show quite rough edges. The water content of PVP measured by TG ranges from 10.5 to 12.5% depending on the relative humidity of the atmosphere above the sample, the lowest value being referred to the measurement performed under dry nitrogen (i.e. with relative humidity $\approx$0%) because some water is lost during sample handling before recording mass, while the highest value is obtained in wet nitrogen when the sample rehydrates. At $\approx$150 °C a slightly sloping trend sets up in the TG curve that is due to a slow decomposition process taking place in such a temperature range. Also the broad endothermic DSC peak associated with water loss changes with the relative humidity of the atmosphere above the sample in the DSC cell: so, at 2 K min^{-1}, the peak ends at 60 °C in dry nitrogen, while the same peak only ends at 110 °C in wet nitrogen. Its enthalpy value is not correctly measurable due to the lack of a long enough baseline before the peak to perform its integration.

High energy milling of pure PVP causes the break-down of the original spherical particles and the mass loss recorded in TG increases due to moisture intake during milling. No significant changes are evident in the DSC trace of pure milled PVP.

Magnesium stearate

The magnesium stearate powder is constituted by thin flakes of irregular shape welded in clusters not bigger than 50 μm (Fig. 4a). The DSC curve (Fig. 5) shows, on heating, the following events: a broad endothermic hump corresponding to the loss of a small amount ($\approx -0.5\%$ in mass from the correspondent TG run) of surface water; two, partially overlapping, DSC broad peaks corresponding to the loss of structural water ($\approx -4.0\%$ in mass from the correspondent TG run); a peak at 110 °C due to the melting of magnesium stearate followed by a minor endothermic peak due to the melting of magnesium palmitate (often present as impurity in commercial lots of magnesium stearate); melting of pseudo-polymorphs of magnesium stearate and magnesium palmitate above 140 °C. The shape of the DSC curve sensibly depends on experimental conditions such as heating rate and relative humidity in the

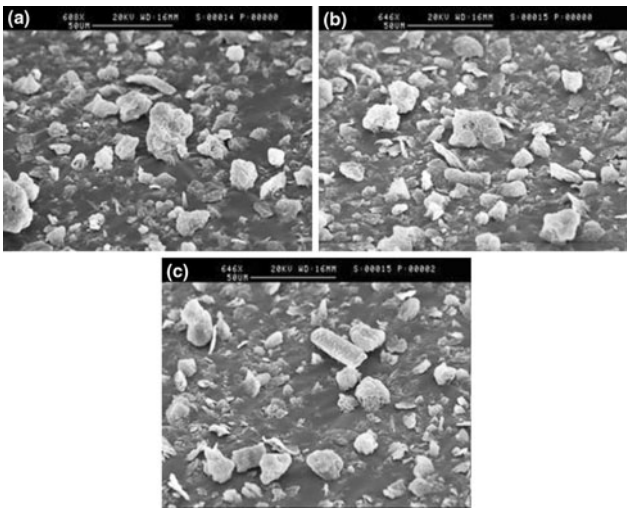

Fig. 4 SEM pictures of magnesium stearate (**a**), haloperidol: magnesium stearate = 20:80 (**b**) and haloperidol: magnesium stearate = 80:20 (**c**)

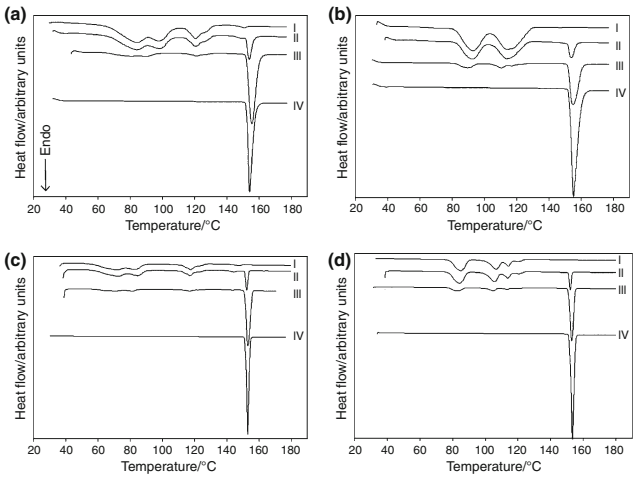

Fig. 5 DSC curves of the system haloperidol:magnesium stearate at 10 K min^{-1} in dry nitrogen (**a**), at 10 K min^{-1} in wet nitrogen (**b**), at 2 K min^{-1} in dry nitrogen (**c**) and at 2 K min^{-1} in wet nitrogen (**d**). Curve I: magnesium stearate; curve II: mixture haloperidol:magnesium stearate = 20:80; curve III: mixture haloperidol: magnesium stearate = 80:20; curve IV: haloperidol

DSC cell: namely the temperature and the shape of the peaks due to the dehydration are both affected by these parameters. Because of the overlapping of dehydration and melting phenomena and the consequent complexity of the thermal traces, we decided to characterize the thermal behaviour of magnesium stearate by reporting the overall enthalpy change (in the temperature range 50–140 °C): the mean value of 237.4 $\pm$ 4.1 J g^{-1} has been obtained independently of heating rate and of relative humidity atmosphere.

α-Lactose monohydrate

The α-lactose powder is constituted by granules with irregular shape and size (Fig. 6a). TG results show that it contains 5% in mass of water, which corresponds to the water content expected for the monohydrate form. Indeed the DSC curve (Fig. 7) shows a broad endothermic peak, with a shoulder towards low temperature, that is reasonably due to such water loss. This peak is followed by an endothermic–exothermic effect at about 170 °C. The endothermic component can be assigned to melting of the unstable form of the anhydrous α-lactose that is the product, besides the stable form of the anhydrous α-lactose, of the dehydration of the hydrate crystals. The exothermic component can be assigned instead to the crystallization of the β:α-lactose compound (1:1 molar). Clearly the determination of the melting enthalpy is not possible so that we decided to characterize the thermal behaviour of α-lactose monohydrate by reporting the enthalpy change of the dehydration peak. It is 155.8 ± 7.6 J g^{-1} with runs at heating rate of 10 K min^{-1} and is 176.1 ± 3.6 J g^{-1} at 2 K min^{-1}. No sensible influence of relative humidity of DSC cell has to be reported.

After milling, the thermal effects are shifted to low temperatures, especially when β is 2 K min^{-1}; the dehydration enthalpy values become 141.6 ± 6.3 J g^{-1} in dry nitrogen and 168.0 ± 0.3 J g^{-1} in wet nitrogen atmosphere at both heating rate.

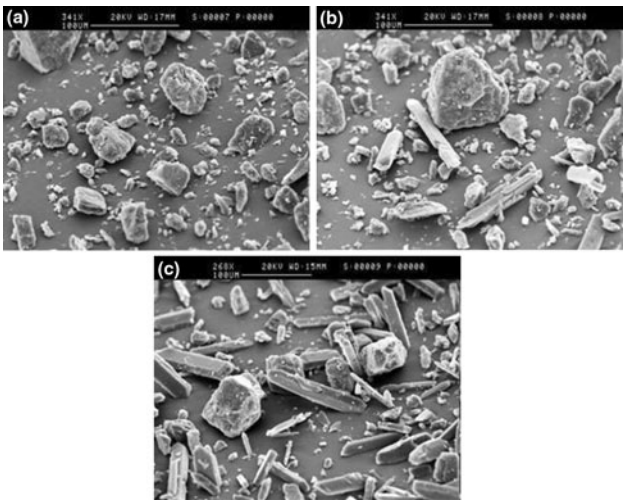

Fig. 6 SEM pictures of α-lactose (**a**), haloperidol:α-lactose = 20:80 (**b**) and haloperidol:α-lactose = 80:20 (**c**)

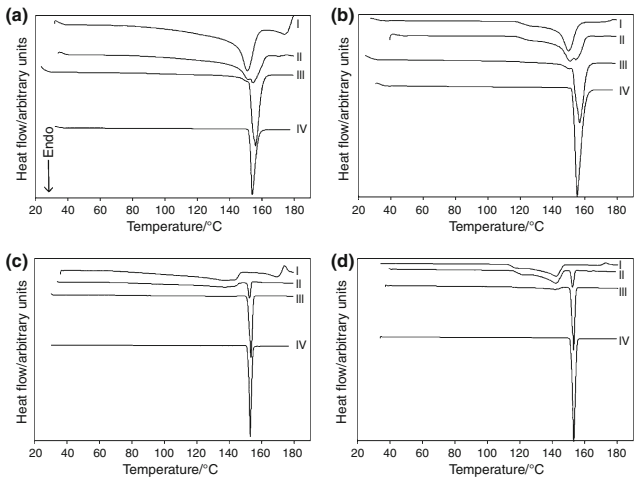

Fig. 7 DSC curves of the system haloperidol:α-lactose at 10 K min^{-1} in dry nitrogen (**a**), at 10 K min^{-1} in wet nitrogen (**b**), at 2 K min^{-1} in dry nitrogen (**c**) and at 2 K min^{-1} in wet nitrogen (**d**). Curve I: α-lactose; curve II: mixture haloperidol:α-lactose = 20:80; curve III: mixture haloperidol:α-lactose = 80:20; curve IV: haloperidol

Binary systems

Haloperidol:PVP system

Haloperidol:PVP = 20:80 Positive indicators of interactions come from both DSC and TG runs. Namely:

(a) the melting peak of haloperidol (Fig. 2) is broader than in the pure drug and its onset temperature is lowered, respectively, to 135.3 °C (β = 10 K min^{-1}) and to 128.9 °C (β = 2 K min^{-1}). Furthermore, a 38% decrease of the mean melting enthalpy is recorded with respect to the value calculated on the basis of the melting enthalpy of pure haloperidol (Table 1);
(b) the sloping trend of the TG baseline that begins, in pure haloperidol, at 150 °C, can be observed at 130 °C in the TG curve of the physical mixture.

On the contrary no clear-cut interaction evidence has been obtained from FT-IR, XRD and SEM experiments. Indeed the FT-IR spectrum of the mixture does not show clearly the peaks and the bands characteristic of the drug that are embedded in the spectral features of the excipient. The XRD peaks of the drug are all present in the pattern of the mixture: simply there are differences in their relative intensities with respect to the patterns of pure drug. SEM micrographs (Fig. 1) do not show any interaction evidence.

Table 1 Calorimetric data of the system haloperidol:PVP

Haloperidol:PVP system composition	$\Delta H_{experimental}$/J g^{-1}	$\Delta H_{expected}$/J g^{-1}
20:80	18.3 ± 0.5	29.7
80:20	97.0 ± 2.0	118.7

The melting parameters attributable to haloperidol change even more in the DSC trace of the milled mixture (Fig. 3): the onset temperature has become 108.2 °C (at $\beta = 10$ K min^{-1}) and 104.0 °C (at $\beta = 2$ K min^{-1}) and moreover the enthalpy change is only 12% of the expected value calculated on the basis of the melting enthalpy of the drug subjected to high energy milling too.

On the contrary, the FT-IR and XRD spectra of the ball-milled mixture are the sum of the effects typical of the milled pure components. The SEM pictures show aggregates in which it is not possible to distinguish the particles of the drug and those of the excipient.

Haloperidol:PVP = 80:20 The melting peak of haloperidol shows a low temperature shoulder (Fig. 2). The onset temperature of such a shoulder corresponds to that of the peak present in the mixture 20:80. The total enthalpy change is about 18% lower than expected in case of no interaction between components (Table 1). The TG analyses do not show any evidence of interaction, i.e. the mass losses are those expected for the amount of PVP in the mixture.

The FT-IR spectrum corresponds to the weighted sum of the signals of the pure components. The XRD pattern shows all the peaks expected for the drug: however, their relative intensities are somewhat changed. No interaction evidence is apparent from SEM micrographs (Fig. 1).

After milling: the low temperature shoulder associated to the main endothermal effect is significantly anticipated (Fig. 3); the total enthalpy is about 17% lower than the value expected for the mixture prepared with milled haloperidol. The FT-IR and XRD spectra of the milled mixture present the effects of the milled pure components. The particles of drug and excipient are no more distinguishable at the SEM analysis. Thus, it seems that the effect of milling vanishes in the case of the 80:20 mixture. Here the drug content of the mixture is higher and plays a deciding role in absorbing itself the mechanical energy rather than converting such a mechanical energy to the interaction process.

Summarizing, clear signals of interaction are found for the haloperidol:PVP system from thermal measurements. The interaction is also more evident as a consequence of milling with the composition 20:80.

Haloperidol:magnesium stearate system

Haloperidol:magnesium stearate = 20:80 In the DSC curves of the physical mixture the thermal effects of both pure components are present and the characteristic temperatures and the enthalpic change values are those expected in case of no interaction (Fig. 5; Table 2). A good agreement between experimental and expected values is obtained also with the thermogravimetric data. The FT-IR and XRD spectra look like the sum of the pure components spectra. SEM pictures (Fig. 4) do not show any interaction evidence.

Haloperidol:magnesium stearate = 80:20 Also for this composition no evidences of interaction are observed (Figs. 4, 5; Table 2).

The results put into evidence that haloperidol is compatible with magnesium stearate.

Haloperidol:α-lactose system

Haloperidol:α-lactose = 20:80 The calorimetric curve shows the thermal effects of both pure components in the respective experimental conditions (Fig. 7). When $\beta = 10$ K min^{-1}, the drug melting and the excipient dehydration partially overlap and the total enthalpic change is compared with the weighted mean of the ΔH values measured for the pure components (Table 3). At 2 K min^{-1} the effects are well separated but the melting peak of haloperidol shows an exothermal return that does not allow a correct integration. In this case only the dehydration peak can be considered for a quantitative comparison. Negative quantitative interaction indicators are obtained for both the heating

Table 3 Calorimetric data of the system haloperidol:α-lactose

Haloperidol:α-lactose system composition	$\Delta H_{experimental}$/ J g^{-1}	$\Delta H_{expected}$/ J g^{-1}
10 K min^{-1}, melting + dehydration		
20:80	159.8 ± 7.9	154.3
80:20	144.2 ± 4.4	149.9
2 K min^{-1}, dehydration		
20:80	144.5 ± 5.6	140.9
80:20	34.5 ± 1.4	35.2

Table 2 Calorimetric data of the system haloperidol:magnesium stearate

Haloperidol:magnesium stearate System composition	Magnesium stearate		Haloperidol	
	$\Delta H_{experimental}$/J g^{-1}	$\Delta H_{expected}$/J g^{-1}	$\Delta H_{experimental}$/J g^{-1}	$\Delta H_{expected}$/J g^{-1}
20:80	188.1 ± 6.8	189.9	29.7 ± 0.8	29.7
80:20	48.7 ± 1.3	47.5	117.5 ± 1.9	118.7

rates. The mass change measured by thermogravimetry agrees with the value expected in case of no interaction. FT-IR, XRD and SEM (Fig. 6) do not suggest interaction.

Thermal, spectroscopic and diffractometric evidences show that the ball-milling does not cause any interaction between the components (Fig. 8). The SEM pictures show aggregates in which it is not possible to distinguish the particles of the drug and those of the excipient.

Haloperidol:α-lactose = 80:20 For the physical mixture of this composition, the same remarks shown for mixture 20:80 are true (Figs. 6 and 7).

It can be claimed that in the system haloperidol-α-lactose monohydrate there is compatibility between components.

Ternary Systems

Haloperidol:PVP:magnesium stearate system

Haloperidol:PVP:magnesium stearate = 20:40:40 The SEM picture (Fig. 9a) shows haloperidol and PVP particles mostly covered by magnesium stearate flakes. The contribution of all the components is identifiable in the DSC curve of the ternary mixture (Fig. 10). When $\beta = 2$ K min^{-1}, the peak attributable to haloperidol melting is 10° below the expected value. The measured melting enthalpies, in all experimental conditions, are lower (Table 4) than the expected ones (by more than 29% for measurements in dry nitrogen and by 36% in wet nitrogen). The degree of interaction is of about the same order than the one measured for the binary system haloperidol:PVP.

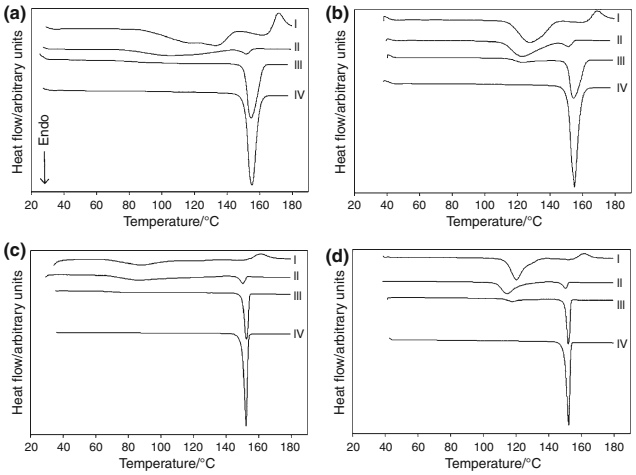

Fig. 8 DSC curves of the milled system haloperidol:α-lactose at 10 K min^{-1} in dry nitrogen (**a**), at 10 K min^{-1} in wet nitrogen (**b**), at 2 K min^{-1} in dry nitrogen (**c**) and at 2 K min^{-1} in wet nitrogen (**d**).Curve I: BM α-lactose; curve II: BM mixture haloperidol:α-lactose = 20:80; curve III: BM mixture haloperidol:α-lactose = 80:20; curve IV: BM haloperidol

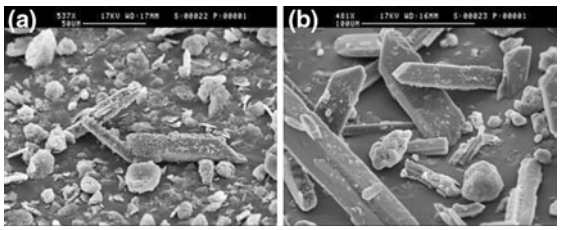

Fig. 9 SEM pictures of haloperidol:PVP:magnesium stearate = 20:40:40 (**a**) and haloperidol:PVP:magnesium stearate = 80:10:10 (**b**)

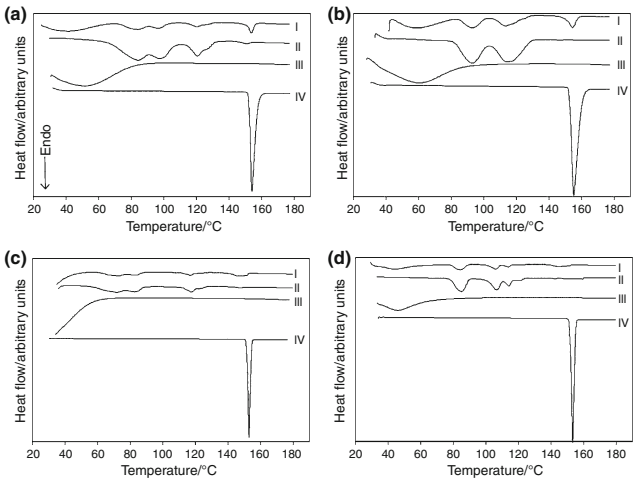

Fig. 10 DSC curves of the system haloperidol:PVP:magnesium stearate = 20:40:40 at 10 K min^{-1} in dry nitrogen (**a**), at 10 K min^{-1} in wet nitrogen (**b**), at 2 K min^{-1} in dry nitrogen (**c**) and at 2 K min^{-1} in wet nitrogen (**d**). Curve I: mixture haloperidol:PVP:magnesium stearate = 20:40:40; curve II: magnesium stearate; curve III: PVP; curve IV: haloperidol

The peaks of magnesium stearate are reduced by at least 28%. The mass loss recorded is slightly lower than the expected value. The FT-IR spectrum is similar to that of magnesium stearate and the peaks of the other components are not seen. No XRD anomalies are noted.

Haloperidol:PVP:magnesium stearate = 80:10:10 The SEM micrograph shows the magnesium stearate flakes attached to the particles of the other components (Fig 9b). The thermal behaviour of the mixture 80:10:10 is additive only from a qualitative point of view (Fig. 11). Quantitatively the peaks of magnesium stearate are reduced by 30% and that of haloperidol by 11% in dry nitrogen and by 16% in wet nitrogen (Table 4). No evidence of interaction emerges from TG data. FT-IR and XRD are those predicted by no interaction hypothesis.

Thus, the thermal measurements suggest that the presence of magnesium stearate does not increase the interaction between haloperidol and PVP, while the presence of PVP affects the behaviour of magnesium stearate (considerable decrease in its DSC peaks intensity).

Table 4 Calorimetric data of the system haloperidol:PVP:magnesium stearate

System composition	Magnesium stearate		Haloperidol	
	$\Delta H_{experimental}$/J g^{-1}	$\Delta H_{expected}$/J g^{-1}	$\Delta H_{experimental}$/J g^{-1}	$\Delta H_{expected}$/J g^{-1}
20:40:40	57.2 ± 5.3	95.0	21.0 ± 1.1	29.7
80:10:10	16.5 ± 0.8	23.7	105.0 ± 2.9	118.7

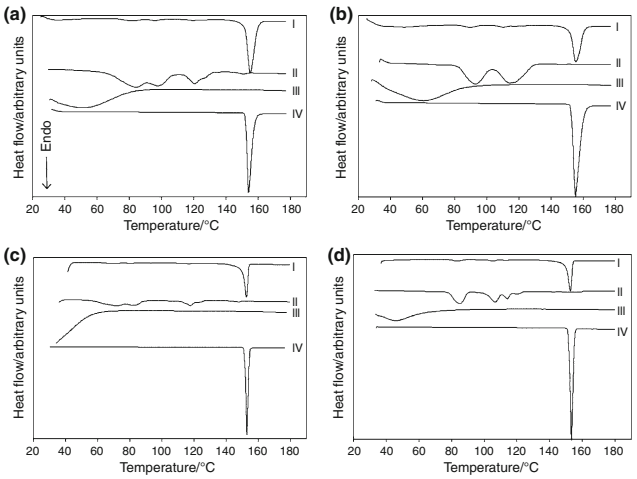

Fig. 11 DSC curves of the system haloperidol:PVP:magnesium stearate = 80:10:10 at 10 K min^{-1} in dry nitrogen (**a**), at 10 K min^{-1} in wet nitrogen (**b**), at 2 K min^{-1} in dry nitrogen (**c**) and at 2 K min^{-1} in wet nitrogen (**d**). Curve I: mixture haloperidol:PVP: magnesium stearate = 80:10:10; curve II: magnesium stearate; curve III: PVP; curve IV: haloperidol

Haloperidol:PVP:α-lactose monohydrate system

Haloperidol:PVP:α-lactose monohydrate = 20:40:40 The SEM analysis suggests that the small α-lactose particles are adherent to those of haloperidol and PVP (Fig. 12a). In the calorimetric curve of the mixture, the dehydration peak of α-lactose monohydrate and that of haloperidol melting partially overlaps (Fig. 13). The total enthalpy of the resulting signal is compared with the weighted mean of the enthalpies of pure components. The difference between the expected and measured values is of the order of 25% (Table 5). The TG curve records two steps of mass loss: the first one, caused by dehydration of PVP, ends within 90 °C and the second one, due to α-lactose monohydrate, is in the 100–160 °C range. The mass changes measured in both steps are those predicted by the no interaction hypothesis. No evidence of interaction is seen in FT-IR and XRD data.

As a consequence of milling, the total enthalpy change measured for the effects of the α-lactose dehydration and haloperidol melting is reduced by about 30% with respect to the value expected for the mixture of the milled pure components (Fig. 14). Negative quantitative interaction indicators are obtained from FT-IR and XRD. The SEM pictures show aggregates in which it is not possible to distinguish the particles of the components.

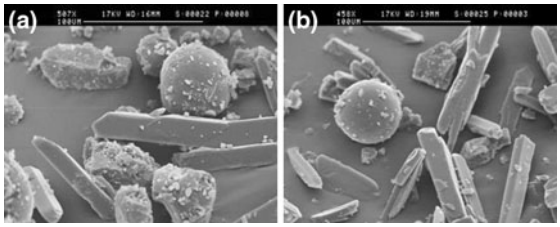

Fig. 12 SEM pictures of haloperidol:PVP:α-lactose = 20:40:40 (**a**) and haloperidol:PVP:α-lactose = 80:10:10 (**b**)

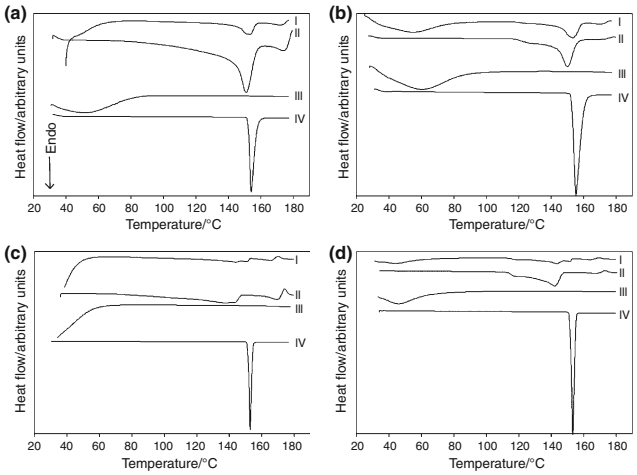

Fig. 13 DSC curves of the system haloperidol:PVP:α-lactose = 20:40:40 at 10 K min^{-1} in dry nitrogen (**a**), at 10 K min^{-1} in wet nitrogen (**b**), at 2 K min^{-1} in dry nitrogen (**c**) and at 2 K min^{-1} in wet nitrogen (**d**). Curve I: mixture haloperidol:PVP:α-lactose = 20:40:40; curve II: α-lactose; curve III: PVP; curve IV: haloperidol

Table 5 Calorimetric data of the system haloperidol:PVP:α-lactose

System composition	$\Delta H_{experimental}$/J g^{-1}	$\Delta H_{expected}$/J g^{-1}
10 K min^{-1}		
20 :40 :40	71.0 ± 4.0	92.0
80:10:10	105.9 ± 0.5	134.3
2 K min^{-1}		
20:40:40	73.3 ± 2.9	100.1
80:10:10	102.1 ± 0.6	136.3

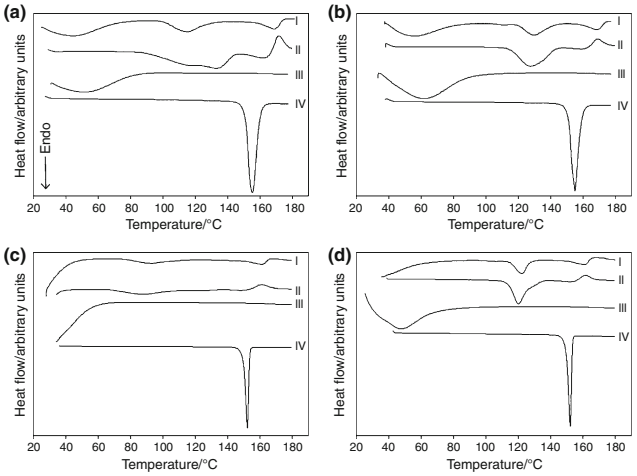

Fig. 14 DSC curves of the milled system haloperidol:PVP:α-lactose = 20:40:40 at 10 K min^{-1} in dry nitrogen (**a**), at 10 K min^{-1} in wet nitrogen (**b**), at 2 K min^{-1} in dry nitrogen (**c**) and at 2 K min^{-1} in wet nitrogen (**d**). Curve I: BM haloperidol:PVP:α-lactose = 20:40:40; curve II: BM α-lactose; curve III: BM PVP; curve IV: BM haloperidol

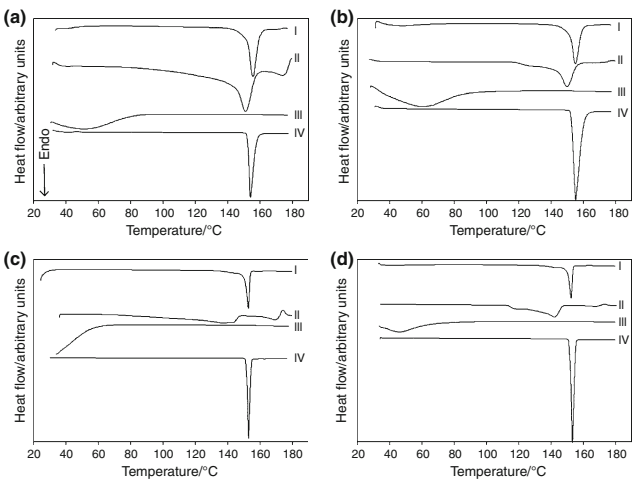

Fig. 15 DSC curves of the system haloperidol:PVP:α-lactose = 80:10:10 at 10 K min^{-1} in dry nitrogen (**a**), at 10 K min^{-1} in wet nitrogen (**b**), at 2 K min^{-1} in dry nitrogen (**c**) and at 2 K min^{-1} in wet nitrogen (**d**). Curve I: mixture haloperidol:PVP:α-lactose = 80:10:10; curve II: α-lactose; curve III: PVP; curve IV: haloperidol

Haloperidol:PVP:α-lactose monohydrate = 80:10:10 For the physical mixture of this composition, the same remarks shown for mixture 20:40:40 are true (Figs. 12b, 15 and 16; Table 5).

In the milled mixture the difference between the enthalpy change measured and expected is about 15%.

The study of this ternary system suggests that the presence of α-lactose does not induce further interaction with respect to that observed in the binary system haloperidol:PVP.

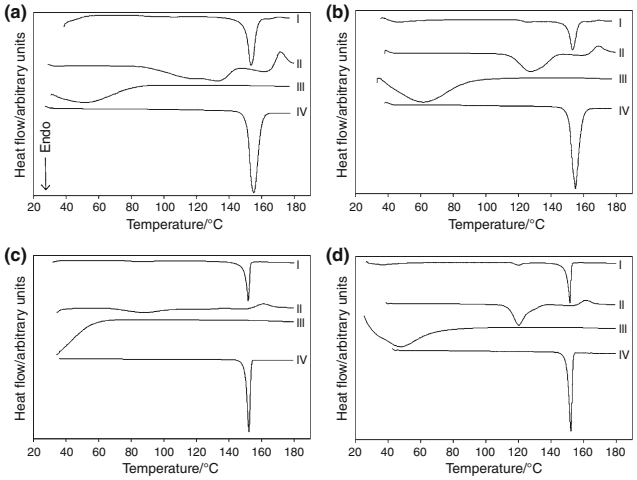

Fig. 16 DSC curves of the milled system haloperidol:PVP:α-lactose = 80:10:10 at 10 K min^{-1} in dry nitrogen (**a**), at 10 K min^{-1} in wet nitrogen (**b**), at 2 K min^{-1} in dry nitrogen (**c**) and at 2 K min^{-1} in wet nitrogen (**d**). Curve I: BM haloperidol:PVP:α-lactose = 80:10:10; curve II: BM α-lactose; curve III: BM PVP; curve IV: BM haloperidol

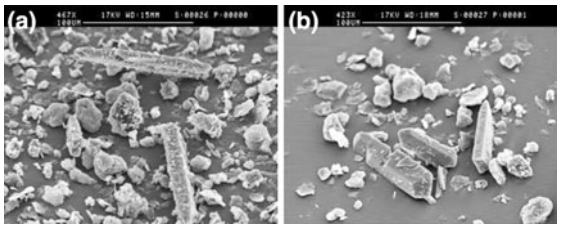

Fig. 17 SEM pictures of haloperidol:magnesium stearate:α-lactose = 20:40:40 (**a**) and haloperidol:magnesium stearate:α-lactose = 80:10:10 (**b**)

Haloperidol:magnesium stearate:α-lactose monohydrate system

Haloperidol:magnesium stearate:α-lactose monohydrate = 20:40:40 The SEM micrograph shows the haloperidol crystals covered by the magnesium stearate and α-lactose monohydrate particles (Fig. 17a).

In the DSC curve of the ternary mixture the effects typical of pure components overlap (Fig. 18) and the total enthalpy perfectly agrees with the weighted mean of the values of pure components (Table 6). The TG data too are those predicted by the no interaction hypothesis. No evidence of interaction is seen in FT-IR and XRD patterns.

Haloperidol:magnesium stearate:α-lactose monohydrate 80:10:10 For this composition, the same remarks shown for mixture 20:40:40 are true (Figs. 17b and 19; Table 6).

It can be claimed that haloperidol is compatible with the concurrent presence of magnesium stearate and α-lactose.

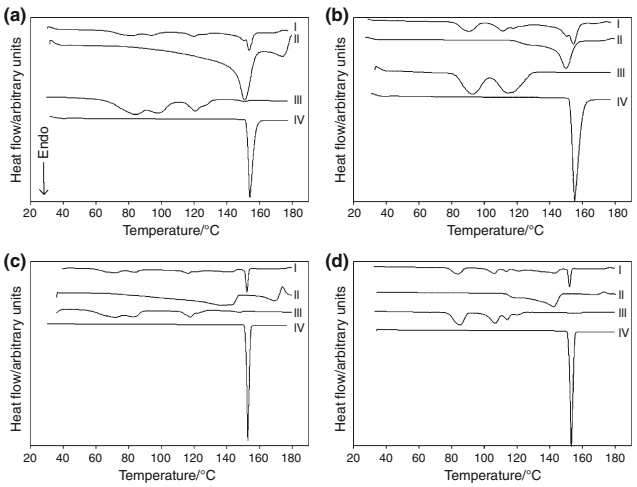

Fig. 18 DSC curves of the milled system haloperidol:magnesium stearate:α-lactose = 20:40:40 at 10 K min^{-1} in dry nitrogen (**a**), at 10 K min^{-1} in wet nitrogen (**b**), at 2 K min^{-1} in dry nitrogen (**c**) and at 2 K min^{-1} in wet nitrogen (**d**). Curve I: mixture haloperidol:magnesium stearate:α-lactose = 20:40:40; curve II: α-lactose; curve III: magnesium stearate; curve IV: haloperidol

Table 6 Calorimetric data of the system haloperidol:magnesium stearate:α-lactose

Composition	$\Delta H_{experimental}$/J g^{-1}	$\Delta H_{expected}$/J g^{-1}
10 K min^{-1}		
20:40:40	176.8 ± 4.2	187.1
80:10:10	156.9 ± 1.8	158.4
2 K min^{-1}		
20:40:40	198.8 ± 7.8	195.1
80:10:10	157.9 ± 4.5	160.7

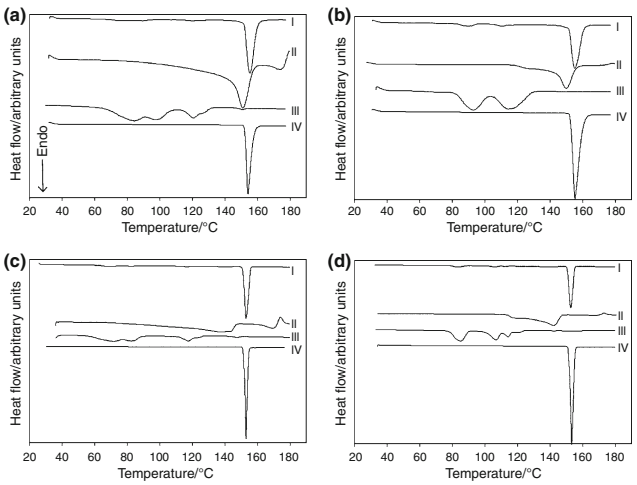

Fig. 19 DSC curves of the milled system haloperidol:magnesium stearate:α-lactose = 80:10:10 at 10 K min^{-1} in dry nitrogen (**a**), at 10 K min^{-1} in wet nitrogen (**b**), at 2 K min^{-1} in dry nitrogen (**c**) and at 2 K min^{-1} in wet nitrogen (**d**). Curve I: mixture haloperidol:magnesium stearate:α-lactose = 80:10:10; curve II: α-lactose; curve III: magnesium stearate; curve IV: haloperidol

Conclusions

A broad range of analytical techniques has been applied to the study of binary and ternary mixtures containing haloperidol as model drug. The analyses have been carried out on both drug-poor and drug-rich mixtures and on untreated and ball-milled mixtures in order to investigate the influence of the system composition and of the mechanical stress on the interaction between the components. As in our previous works [8–11], also in this case the DSC has proven to be, among the selected analytical techniques, the most sensitive and specific in picking out interaction indicators. The utility of this technique is related also to its capacity to provide quantitative indicators in addition to qualitative indicators. Our measurements put into evidence that PVP interacts with haloperidol. The interaction is favoured by the mechanical stress and is more evident in the composition 20:80. On the contrary, α-lactose and magnesium stearate were found to be compatible with the drug.

References

1. Antipas AS, Landis MS. Solid-state excipient compatibility testing. Drugs Pharm Sci. 2005;153:419–58.
2. Kiss D, Zelko R, Novak Cs, Ehen Zs. Application of DSC and NIRS to study the compatibility of metronidazole with different pharmaceutical excipients. J Therm Anal Calorim. 2006;84:447–51.
3. Corvi Mora P, Cirri M, Mura P. Differential scanning calorimetry as a screening technique in compatibility studies of DHEA extended release formulations. J Pharm Biomed Anal. 2006;42:3–10.
4. Desay SR, Shaikh MM, Dharwadkar SR. Preformulation compatibility studies of etamsylate and fluconazole drugs with lactose by DSC. J Therm Anal Calorim. 2003;71:651–8.
5. Stulzer HK, Rodrigues PO, Cardoso TM, Matos JSR, Silvia MAS. Compatibility studies between captopril and pharmaceutical excipients used in tablets formulations. J Therm Anal Calorim. 2008;91:323–8.
6. Laszcz M, Kosmacinska B, Korczak K, Smigielska B, Glice M, Maruszak W, et al. Study on compatibility of imatinib mesylate with pharmaceutical excipients. J Therm Anal Calorim. 2007;88:305–10.
7. Cunha-Filho MSS, Martìnez-Pacheco R, Landìn M. Compatibility of the antitumoral β-lapachone with different solid dosage forms excipients. J Pharm Biomed Anal. 2007;45:590–8.
8. Bruni G, Amici L, Berbenni V, Marini A, Orlandi A. Drug-excipient compatibility studies Search of interaction indicators. J Therm Anal Calorim. 2002;68:561–73.
9. Marini A, Berbenni V, Moioli S, Bruni G, Cofrancesco P, Margheritis C, et al. Drug-excipient compatibility studies by physico-chemical techniques The case of indomethacin. J Therm Anal Calorim. 2003;73:529–45.
10. Marini A, Berbenni V, Pegoretti M, Bruni G, Cofrancesco P, Sinistri C, et al. Drug-excipient compatibility studies by physico-chemical techniques The case of atenolol. J Therm Anal Calorim. 2003;73:529–45.
11. Marini A, Berbenni V, Bruni G, Cofrancesco P, Giordano F, Villa M. Physico-chemical characterization of drugs and drug forms in the solid state. Curr Med Chem. 2003;2:303–21.